same steps have to be repeated, the process will be slower or distortion will result. Examining the sublimation of $(SN)_x$, by photoionization mass spectrometry, Lau et al.[11] found only S_3N_3, and no S_2N_2 or SN, probably due to the low photon energy (10.2 eV) used (see our Figure 3—the energy dependence of the mass spectrum).

The polymerization process itself appears to have two important steps; the first is the fragmentation to S_2N_2, and the second is the transformation of S_2N_2 to $(SN)_2$. Both are facilitated by using higher temperatures or catalysts. At the same time, increasing the temperature may lead to side reactions involving loss of N. The quantity of $(SN)_2$ is critical; if there is "too much" during the reaction, the polymer quality will be degraded. From Figure 6 it is clear that the best way to obtain the polymer is to use a small amount of $(SN)_2$ and to move the $S_2N_2 \rightarrow SN$ equilibrium in favor of SN.

Conclusions

On the basis of thermal decomposition of S_4N_4 over and in the absence of silver wool, as well as considering appearance potentials of different mass spectral fragments originating from S_4N_4 and S_2N_2, we propose a mechanism for the $(SN)_x$ polymerization process. This mechanism explains some conflicting observations reported by previous workers and includes two important steps—the fragmentation of S_4N_4 to S_2N_2 and the transformation of S_2N_2 to $(SN)_2$. Both steps are facilitated by increasing the temperature, which also results in nitrogen atom loss. In the first step the large surface of different wools brings quick quasi-equilibrium; the second is affected by temperature and/or the presence of silver wool as a catalyst. The polymerization process involves the reaction of $(SN)_2$ with SN originating from S_2N_2.

Acknowledgment. This work was supported by grants from the NSERC of Canada. We are grateful to Professor N. L. Paddock for the starting material S_4N_4 and for many stimulating discussions.

Registry No. S_4N_4, 28950-34-7; Ag, 7440-22-4; S_2N_2, 25474-92-4; $(SN)_x$, 56422-03-8.

Contribution from the Department of Chemistry, Florida Atlantic University, Boca Raton, Florida 33431

Electrochemical Reduction of Seven-Coordinate Oxomolybdenum(VI) Complexes. Multielectron Transfer at Mononuclear MoO^{4+} Centers

Julie R. Bradbury[1] and Franklin A. Schultz*

Received May 22, 1986

The seven-coordinate oxomolybdenum(VI) complexes $MoOX_2(S_2CNEt_2)_2^{n+}$ (X_2 = $2Cl^-$, $2Br^-$, catecholate (cat) (n = 0); X_2 = $Et_2NCS_2^-$ (n = 1)) undergo two-electron electrochemical reduction in nonaqueous solvents. Changes in Mo coordination number accompany electron transfer and provide the driving force for multielectron behavior. Evidence suggests that one metal–ligand bond is broken in conjunction with each electron addition and that the pathway of electrochemical reduction is seven-coordinate Mo(VI) → six-coordinate Mo(V) → five-coordinate Mo(IV). Depending on the identity of X_2, this two-electron change appears as either a single two-electron transfer or two closely spaced one-electron transfers. $MoOCl_2(S_2CNEt_2)_2$ is reduced to $MoO(S_2CNEt_2)_2 + 2Cl^-$ in a two-electron step. $MoO(S_2CNEt_2)_2$ is reoxidized to $MoOCl_2(S_2CNEt_2)_2$ in the presence of Cl^-, but at a potential ~1 V more positive than Mo(VI) reduction. Thus, the two-electron interconversion of $MoOCl_2(S_2CNEt_2)_2$ and $MoO(S_2CNEt_2)_2 + 2Cl^-$ is highly irreversible. $MoO(S_2CNEt_2)_2^+$ and $MoO(cat)(S_2CNEt_2)_2$ complexes with electron-withdrawing catechol substituents (Cl_4cat, NO_2cat) exhibit Mo(VI)/Mo(V) and Mo(V)/Mo(IV) reduction waves separated by ~0.2 V. Mo(VI)/Mo(V) reduction is chemically reversible for these tris(bidentate) species because cleavage of one metal–ligand bond does not displace a bidentate ligand from the molecule and the bond is easily re-formed upon reoxidation to Mo(VI). $MoO(cat)(S_2CNEt_2)_2$ complexes with electron-donating substituents (cat, DTBcat) also exhibit separate Mo(VI)/Mo(V) and Mo(V)/Mo(IV) reduction waves, but a rapid chemical reaction following the first charge transfer causes more than one electron to be transferred at the potential of Mo(VI) reduction.

Introduction

The oxomolybdenum(VI) center (MoO^{4+}), which typically exhibits seven-coordinate pentagonal-bipyramid geometry,[2] is becoming an increasingly common structural feature in molybdenum chemistry.[3-11] In contrast to more numerous *cis*-dioxo MoO_2^{2+} complexes, whose redox properties have been widely studied,[12] relatively few electrochemical investigations have been

(1) Current address: Department of Chemistry, Washington University, St. Louis, MO 63130.
(2) (a) Drew, M. G. *Prog. Inorg. Chem.* **1977**, *23*, 67. (b) Melnik, P.; Sharrock, P. *Coord. Chem. Rev.* **1985**, *65*, 49.
(3) (a) Stiefel, E. I. *Prog. Inorg. Chem.* **1977**, *22*, 1. (b) Stiefel, E. I. In *Molybdenum and Molybdenum-Containing Enzymes*; Coughlan, M. P., Ed.; Pergamon: Oxford, England, 1980; Chapter 2.
(4) Dirand, J.; Ricard, L.; Weiss, R. *J. Chem. Soc., Dalton Trans.* **1976**, 278.
(5) Dirand, J.; Ricard, L.; Weiss, R. *Transition Met. Chem. (Weinheim, Ger.)* **1975**, *1*, 2.
(6) Liebeskind, L. S.; Sharpless, K. B.; Wilson, R. D.; Ibers, J. A. *J. Am. Chem. Soc.* **1978**, *100*, 7061.
(7) Chen, G. J.-J.; McDonald, J. W.; Newton, W. E. *Inorg. Chim. Acta* **1980**, *41*, 49.
(8) Wieghardt, K.; Holzbach, W.; Hofer, E.; Weiss, J. *Inorg. Chem.* **1981**, *20*, 343.
(9) Young, C. G.; Broomhead, J. A.; Boreham, C. J. *J. Chem. Soc., Dalton Trans.* **1983**, 2135.
(10) (a) Ricard, L.; Weiss, R. *Inorg. Nucl. Chem. Lett.* **1974**, *10*, 217. (b) Dirand, J.; Ricard, L.; Weiss, R. *Inorg. Nucl. Chem. Lett.* **1975**, *11*, 661.
(11) (a) Newton, W. E.; McDonald, J. W.; Corbin, J. L.; Ricard, L.; Weiss, R. *Inorg. Chem.* **1980**, *19*, 1997. (b) Marabella, C. P.; Enemark, J. H.; Newton, W. E.; McDonald, J. W. *Inorg. Chem.* **1982**, *12*, 623.
(12) (a) Isbell, A. F., Jr.; Sawyer, D. T. *Inorg. Chem.* **1971**, *10*, 2449 (b) DeHayes, L. J.; Faulkner, H. C.; Doub, W. H., Jr.; Sawyer, D. T. *Inorg. Chem.* **1975**, *14*, 2110. (c) Hyde, J.; Venkatasubramanian, K.; Zubieta, J. *Inorg. Chem.* **1978**, *17*, 414. (d) Spence, J. T. In *Molybdenum and Molybdenum-Containing Enzymes*; Coughlan, M. P., Ed.; Pergamon: Oxford, 1980; Chapter 3. (e) Cliff, C. A.; Fallon, G. D.; Gatehouse, B. M.; Murray, K. S.; Newman, P. J. *Inorg. Chem.* **1980**, *19*, 773. (f) Charney, L. M.; Schultz, F. A. *Inorg. Chem.* **1980**, *19*, 1527. (g) Rajan, O. A.; Chakravorty, A. *Inorg. Chem.* **1981**, *20*, 660. (h) Topich, J. *Inorg. Chem.* **1981**, *20*, 3704. (i) Lamache, M.; Sanbuichi, F. *Electrochim. Acta* **1981**, *26*, 1525. (j) Charney, L. M.; Finklea, H. O.; Schultz, F. A. *Inorg. Chem.* **1982**, *21*, 549. (k) Pickett, C.; Kumar, S.; Vella, P. A.; Zubieta, J. *Inorg. Chem.* **1982**, *21*, 908. (l) Ghosh, P.; Chakravorty, A. *Inorg. Chem.* **1983**, *22*, 1322. (m) Rajan, O. A.; Spence, J. T.; Leman, C.; Minelli, M.; Sato, M.; Enemark, J. H.; Kroneck, P. M. H.; Sulger, K. *Inorg. Chem.* **1983**, *22*, 3065. (n) Chaudhury, M. *J. Chem. Soc., Dalton Trans.* **1984**, 115. (o) Ledon, H.; Varescon, F.; Malinski, T.; Kadish, K. M. *Inorg. Chem.* **1984**, *23*, 261. (p) Subramanian, P.; Spence, J. T.; Ortega, R.; Enemark, J. H. *Inorg. Chem.* **1984**, *23*, 2564. (q) Bristow, S.; Garner, C. D.; Pickett, C. J. *J. Chem. Soc., Dalton Trans.* **1984**, 1617. (r) Corbin, J. L.; Miller, K. F.; Pariyadath, N.; Wherland, S.; Bruce, A. E.; Stiefel, E. I. *Inorg. Chim. Acta* **1984**, *90*, 41. (s) Backes-Dahmann, G.; Hermann, W.; Wieghardt, K.; Weiss, J. *Inorg. Chem.* **1985**, *24*, 485. (t) Berg, J. M.; Holm, R. H. *J. Am. Chem. Soc.* **1985**, *107*, 917. (u) Kaul, B. B.; Enemark, J. H.; Merbs, S. L.; Spence, J. T. *J. Am. Chem. Soc.* **1985**, *107*, 2885.

0020-1669/86/1325-4408$01.50/0

Chart I

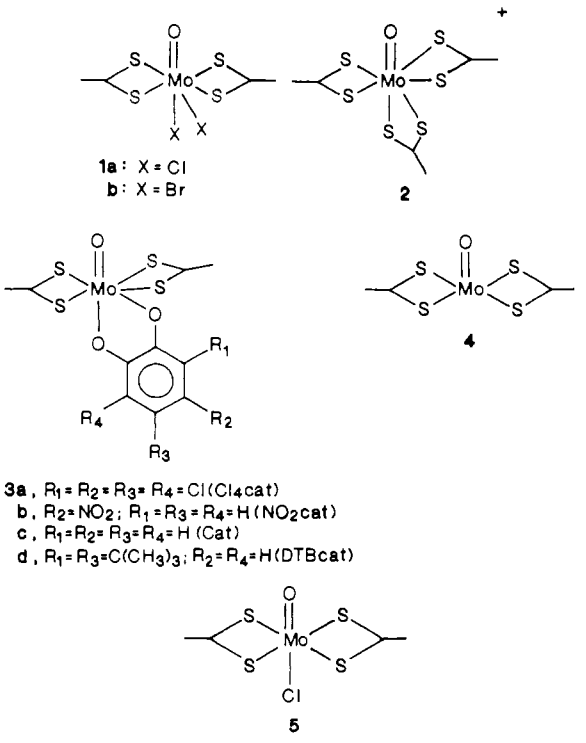

conducted on complexes containing an MoO^{4+} center.[12l,n,13-15] Interest in compounds of both types derives from their relationship to the molybdenum hydroxylases,[16] enzymes that contain oxo functionalities on Mo, cycle among the Mo(VI), -(V), and -(IV) oxidation states, and carry out the equivalent of two-electron oxidation or reduction of their respective substrates.

As part of our program[12f,j,17] to investigate relationships between molecular structure and redox properties of molybdenum-containing compounds, we have undertaken study of the electrochemical reduction of the seven-coordinate complexes $MoOX_2(S_2CNEt_2)_2$ (**1**; X = Cl, Br),[4] $MoO(S_2CNEt_2)_3^+$ (**2**),[5] and $MoO(cat)(S_2CNEt_2)_2$ (**3**)[18,19] (Chart I). X-ray crystallographic structures have been reported for compounds **1a**,[4] **1b**,[4] and **2**.[5] They exhibit pentagonal-bipyramidal geometry with the oxo group located in one axial position and two dithiocarbamate ligands occupying four coordination sites in the equatorial plane about Mo. The remaining coordination sites are occupied by either a third bidentate $Et_2NCS_2^-$ ligand or two monodentate halide ligands. Complexes **3a–d** were prepared recently in our laboratory.[18] Their structures have not been determined, but we assume they adopt a similar geometry with the large-bite-angle catecholate ligand spanning axial and equatorial positions. This structural arrangement has been found[15] in the related seven-coordinate complex $MoO(cat)(ONC_5H_{10})_2$, where $C_5H_{10}NO^-$ is the 1-piperidinolate ligand.

Table I. NPV and CV Current Parameters for One-Electron Redox Systems[a]

solvent	redox couple	i_d/AC, μA cm^{-2} mM^{-1}	$i_p/v^{1/2}AC$, μA $s^{1/2}$ $V^{-1/2}$ cm^{-2} mM^{-1}
CH_3CN	$Mo(S_2CNEt_2)_4^{+/0}$	970	890
DMF	$Mo(S_2C_2(CN)_2)_4^{3-/4-}$	590	545
CH_2Cl_2	$Mo(S_2CNEt_2)_4^{+/0}$	995	885

[a] ±5% in 0.1 M $[Bu_4N]PF_6$ for the indicated redox couple measured as a reduction.

The present paper describes the electrochemical reduction of complexes **1–3** in nonaqueous solvents. We also report on the electrochemical behavior of the related monooxo Mo(IV) and Mo(V) complexes $MoO(S_2CNEt_2)_2$ (**4**)[20] and $MoOCl(S_2CNEt_2)_2$ (**5**).[7] Inclusion of these compounds is helpful in interpreting results for the seven-coordinate MoO^{4+} complexes and allows us to interrelate electrochemical behavior of complexes containing MoO^{4+}, MoO^{3+}, and MoO^{2+} centers. At the outset of this investigation we discovered that these monomeric species participate in multielectron-transfer reactions in nonaqueous aprotic solvents. Our objectives thus became to characterize these processes and to understand the role of the molybdenum coordination environment in the multielectron transfers.

Experimental Section

Materials. The following compounds were prepared by the literature method cited: $MoOCl_2(S_2CNEt_2)_2$,[4] $MoOBr_2(S_2CNEt_2)_2$,[5] $MoOCl(S_2CNEt_2)_2$,[7] $MoO(S_2CNEt_2)_2$,[20c] and $WOCl_2(S_2CNEt_2)_2$.[7] Preparation of the $MoO(cat)(S_2CNEt_2)_2$ complexes (**3a–d**) is described in a subsequent paper.[18] $MoO(S_2CNEt_2)_3^+$ was examined as the BPh_4^- salt, which was prepared by metathesis of $[MoO(S_2CNEt_2)_3]Mo_2O_4F_6$[5] and $NaBPh_4$. In this procedure, sodium tetraphenylborate (0.21 g, 0.6 mmol) was added to $[MoO(S_2CNEt_2)_3]_2Mo_2O_4F_6$ (0.45 g, 0.3 mmol) dissolved in ca. 20 mL of argon-purged CH_2Cl_2 to give an orange, crystalline precipitate of $[MoO(S_2CNEt_2)_3]BPh_4$.

Acetonitrile (CH_3CN), *N*,*N*-dimethylformamide (DMF), and dichloromethane (CH_2Cl_2) solvents were distilled-in-glass reagents from Burdick & Jackson and were stored over dried molecular sieves. Either tetra-*n*-butylammonium hexafluorophosphate ($[Bu_4N]PF_6$) or tetraethylammonium tetrafluoroborate ($[Et_4N]BF_4$) from Southwestern Analytical Chemicals was used as supporting electrolyte; these materials were dried and desiccated before use. Other reagents were commercial materials that were used as received.

Electrochemical Measurements. Cyclic voltammetry (CV) and normal pulse voltammetry (NPV) experiments were conducted with an IBM EC-225 voltammetric analyzer. We employed a three-electrode cell configuration consisting of a Pt-disk working electrode, a Pt-wire auxiliary electrode, and a saturated calomel (SCE) reference electrode. The SCE was separated from the sample solution by a salt bridge containing solvent and supporting electrolyte. The working electrode was either a Beckman 392273 Pt disk (area 0.20 cm^2) or a Bioanalytical Systems MF 2013 Pt disk (area 0.020 cm^2). These geometric areas were determined by optical microscopy and were used to calculate normalized CV and NPV current parameters.

A sweep rate of 4 mV s^{-1} and a pulse repetition time of 2 s were used in NPV experiments. Compounds that undergo irreversible charge transfer exhibit a peak-shaped response owing to depletion effects when examined at stationary electrodes by this technique.[21] To alleviate this

(13) Chrichton, B. A. L.; Dilworth, J. R.; Pickett, C. J. *J. Chem. Soc., Dalton Trans.* **1981**, 419.
(14) (a) Ghosh, P.; Bandyopadhyay, P.; Chakravorty, A. *J. Chem. Soc., Dalton Trans.* **1983**, 401. (b) Chaudhury, M. *Inorg. Chem.* **1984**, *23*, 4434.
(15) Bristow, S.; Enemark, J. H.; Garner, C. D.; Minelli, M.; Morris, G. A.; Ortega, R. B. *Inorg. Chem.* **1985**, *24*, 4070.
(16) Access to much of the literature on the structure, function, and chemical modeling of these enzymes may be obtained through the following references: (a) Bray, R. C. *Enzymes (3rd Ed.)* **1975**, *12*, 299–419. (b) Spence, J. T. *Coord. Chem. Rev.* **1983**, *48*, 59. (c) Holm, R. H.; Berg, J. M. *Pure Appl. Chem.* **1984**, *56*, 1645.
(17) (a) Schultz, F. A.; Ledwith, D. A.; Leazenbee, L. O. *Electrochemical Studies of Biological Systems*; ACS Symposium Series 38; American Chemical Society: Washington, DC, 1977; p 77. (b) Schultz, F. A. In *Molybdenum Chemistry of Biological Significance*; Otsuka, S., Newton, W. E., Eds.; Plenum: New York, 1980; pp 345–360. (c) Finklea, H. O.; Lahr, S. K.; Schultz, F. A. *Electrochemical and Spectrochemical Studies of Biological Redox Components*; Advances in Chemistry 201; American Chemical Society: Washington, DC, 1982; p 709. (d) Ott, V. R.; Schultz, F. A. *J. Electroanal. Chem. Interfacial Electrochem.* **1975**, *59*, 47. (e) Ott, V. R.; Schultz, F. A. *J. Electroanal. Chem. Interfacial Electrochem.* **1975**, *61*, 81. (f) Ott, V. R.; Swieter, D. S.; Schultz, F. A. *Inorg. Chem.* **1977**, *16*, 2538. (g) Schultz, F. A.; Ott, V. R.; Rolison, D. S.; Bravard, D. C.; McDonald, J. W.; Newton, W. E. *Inorg. Chem.* **1978**, *17*, 1758. (h) Smith, D. A.; Schultz, F. A. *Inorg. Chem.* **1982**, *21*, 3035. (i) Smith, D. A.; McDonald, J. W.; Finklea, H. O.; Ott, V. R.; Schultz, F. A. *Inorg. Chem.* **1982**, *21*, 3825. (j) Perkins, P. G.; Schultz, F. A. *Inorg. Chem.* **1983**, *22*, 1133. (k) Lahr, S. K.; Finklea, H. O.; Schultz, F. A. *J. Electroanal. Chem. Interfacial Electrochem.* **1984**, *163*, 257. (l) Zhuang, B.; McDonald, J. W.; Schultz, F. A.; Newton, W. E. *Organometallics* **1984**, *3*, 943.
(18) Bradbury, J. R.; Schultz, F. A. *Inorg. Chem.*, following paper in this issue.
(19) The abbreviations cat^{2-}, $SQ^{\bullet-}$, and Q are used to represent the catecholate, semiquinone, and quinone forms of the catechol ligands.
(20) (a) Jowitt, R. N.; Mitchell, P. C. H. *J. Chem. Soc. A* **1969**, 2631. (b) Newton, W. E.; Corbin, J. L.; Bravard, D. C.; Searles, J. E.; McDonald, J. W. *Inorg. Chem.* **1974**, *13*, 1100. (c) Chen, G. J.-J.; McDonald, J. W.; Newton, W. E. *Inorg. Chem.* **1976**, *15*, 2612.

Table II. Electrochemical Data for Reduction of MoO^{4+} Complexes[a]

		CV		NPV		CPC	
compd	solvent	E_{pc}, V	$i_p/\nu^{1/2}AC$, $\mu A\ s^{1/2}\ V^{-1/2}\ cm^{-2}\ mM^{-1}$	$E_{1/2}$, V	i_d/AC,[b] $\mu A\ cm^{-2}\ mM^{-1}$	E, V	n
$MoOCl_2(S_2CNEt_2)_2$	CH_3CN	−0.2[c]	110[c]	−0.2[c]	160[c]	−0.7	2.06
		−0.43	1550	−0.44	1710 (1870)		
$MoOBr_2(S_2CNEt_2)_2$	CH_3CN	−0.1[c]	440[c]	−0.1[c]	530[c]	−0.6	2.08
		−0.37	1250	−0.35	1440 (1970)		
$MoO(S_2CNEt_2)_3^+$	CH_3CN	−0.31	1460	−0.31	1740	−0.5	0.89
$MoO(Cl_4cat)(S_2CNEt_2)_2$	CH_3CN	−0.50	760	−0.53	940	−1.25	1.75
		−0.69	300	−0.74	550 (1490)		
		−1.50	160	−1.46	350 (1840)		
	DMF	−0.40	510	−0.41	560		
		−0.69	260	−0.74	550 (1110)		
		−1.55	280				
	CH_2Cl_2	−0.60	920	−0.61	1100		
		−0.81	310	−0.89	1090 (2190)		
		−1.43	380				
$MoO(NO_2cat)(S_2CNEt_2)_2$	CH_3CN	−0.59	770	−0.57	950	−1.10	1.77
		−0.73	90	−0.74	550 (1500)		
	DMF	−0.41	520	−0.45	580		
		−0.74	230	−0.76	480 (1060)		
	CH_2Cl_2	−0.62	930	−0.63	990		
		−0.82	170	−0.89	1000 (1990)		
$MoO(Cat)(S_2CNEt_2)_2$	CH_3CN	−0.76	850	−0.76	1380	−1.4	2.16
		−1.06	80	−1.12	520 (1900)		
	CH_2Cl_2	−0.91[d]	1100	−0.89	1680		
				−1.21	500 (2180)		
$MoO(DTBcat)(S_2CNEt_2)_2$	CH_3CN	−0.76[d]	930	−0.76	1380	−1.5	2.09
				−1.15	470 (1850)		
	DMF	−0.67	740	−0.71	1020		
		−1.25	90	−1.24	170 (1190)		
	CH_2Cl_2	−0.88[d]	1330	−1.02[d]	2060 (2060)		

[a] Recorded for 0.3–1.2 mM solutions of complexes in 0.1 M $[Bu_4N]PF_6$; CV sweep rate 0.1 V s^{-1}. [b] The number in parentheses is the total NPV current parameter measured on the limiting current plateau of the indicated wave. [c] Additional wave assigned to solvolyzed species (see text for discussion). The current parameters increase with time; the values given are for solutions ca. 20 min after preparation. [d] Only one reduction wave observed under these conditions.

problem, we agitated the solution with a motor-driven stirrer while recording voltammograms. Stirring serves to replenish the diffusion layer during the resting phase of the pulse but does not disturb concentration profiles near the electrode surface during the brief active interval (ca. 50-ms duration) of the pulse. As a result, limiting current plateaus of normal height and appearance are recorded for irreversible electrode reactions, whereas current–potential curves of reversible reactions are unaltered from quiescent solution behavior. All NPV data were recorded with solutions stirred in this manner.

Controlled-potential coulometry was conducted with an EG&G Princeton Applied Research (PAR) 173/179 potentiostat and digital coulometer using a PAR 377 coulometry cell. The working electrode in these experiments was a 12-cm^2 Pt foil, and the auxiliary electrode was isolated from the working electrode compartment by a glass frit. In many of the coulometry experiments we observed continual accumulation of a small amount of charge near the end of electrolysis. Thus, we calculated the apparent number of electrons transferred from the relation $n_{app} = Q/Fm$, where F is the Faraday constant, m is the moles of material, and Q is the coulomb reading at the time the current dropped to <1–3% of its original value. In the case of $MoO(DTBcat)(S_2CNEt_2)_2$ electrolysis, the current was still 11% of its original value at the time the final coulomb reading was taken.

All electrochemical experiments were carried out at ambient temperature (22 ± 2 °C). Solutions were deoxygenated and blanketed with a stream of argon that had been passed through a tower of solvent and supporting electrolyte.

One-Electron Redox Systems. As an adjunct to coulometric measurements, comparison of voltammetric wave heights is helpful in establishing the number of electrons transferred in an electrode reaction. This is so particularly for NPV, because the limiting current in this technique is independent of the heterogeneous charge-transfer rate and the possible existence of overlapping steps in the redox process. Table I contains NPV and CV current parameters in three solvents for the well-characterized one-electron redox systems $Mo(S_2CNEt_2)_4^{+/0}$ and $Mo[S_2C_2(CN)_2]_4^{3-/4-}$,[17h,i] which we use to help establish the number of electrons transferred. These compounds are suitable for this purpose because they have approximately the same molecular mass as complexes **1–5**.

Results and Discussion

The electrochemical behavior of compounds **1–5** was investigated by cyclic voltammetry (CV), normal pulse voltammetry (NPV), and controlled-potential coulometry (CPC). Study of compounds **1**, **2**, **4**, and **5** was limited to CH_3CN. However, compounds **3a–d** exhibited instances of solvent-dependent behavior and were studied in CH_3CN, DMF, and CH_2Cl_2. Additional data for compounds **3a–d** and the remaining members of a nine-membered series of $MoO(cat)(S_2CNEt_2)_2$ complexes are reported in a subsequent publication.[18]

Electrochemical data for reduction of the MoO^{4+} complexes are reported in Table II. Table III contains data for anticipated electrode reaction products of these species. The latter information is in substantial agreement with earlier investigations of Cl^-,[22,23] Br^-,[23,24] $Et_2NCS_2^-$,[25] and $MoO(S_2CNEt_2)_2$.[12b,c] No previous electrochemistry of $MoOCl(S_2CNEt_2)_2$ has been reported.

Molybdenum(VI) Reduction Potentials. The initial reduction step of the MoO^{4+} complexes occurs at potentials between ca. −0.1 and −0.8 V vs. SCE in CH_3CN. This range lies between the values for reduction of the eight-coordinate non-oxo complex Mo-

(21) (a) Morris, J. L., Jr.; Faulkner, L. R. *Anal. Chem.* **1977**, *49*, 489. (b) Bond, A. M. *Modern Polarographic Methods in Analytical Chemistry*; Marcel Dekker: New York, 1980; pp 267–272.

(22) Miller, L. L.; Katz, M. *J. Electronanal. Chem. Interfacial Electrochem.* **1976**, *72*, 329.

(23) (a) Kolthoff, I. M.; Coetzee, J. F. *J. Am. Chem. Soc.* **1957**, *79*, 1852. (b) Gutman, V.; Duschek, O. *Monatsh. Chem.* **1973**, *104*, 654.

(24) Magno, F.; Mazzocchin, G.; Bontempelli, G. *J. Electroanal. Chem. Interfacial Electrochem.* **1973**, *47*, 461.

(25) (a) Scrimager, C.; DeHayes, L. J. *Inorg. Nucl. Chem. Lett.* **1978**, *14*, 125. (b) Cauquis, G.; Lachenal, D. *J. Electroanal. Chem. Interfacial Electrochem.* **1973**, *43*, 205.

Table III. Voltammetric Data for Anticipated Electrode Reaction Products of MoO^{4+} Complexes[a]

		CV		NPV	
compd	process	E_p, V	$i_p/\nu^{1/2}AC$, $\mu A\ s^{1/2}\ V^{-1/2}\ cm^{-2}\ mM^{-1}$	$E_{1/2}$, V	i_d/AC, $\mu A\ cm^{-2}\ mM^{-1}$
$[Et_4N]Cl$	ox	+1.00	924	+0.95	1074
$[(heptyl)_4N]Br$[b]	ox	+0.69	692	+0.61	880
		+0.98	322	+0.92	420
$Na[S_2CNEt_2]$	ox	+0.01	1060	0.00	1070
$MoO(S_2CNEt_2)_2$	red	−2.1	880	−2.2	1200
	ox	+0.48	990	+0.45	1130
$MoOCl(S_2CNEt_2)_2$[b]	red	−0.39	830	−0.35	1010
	ox	+0.59	580	+0.56	890

[a] Data recorded for 0.9–1.9 mM solutions of compounds in 0.1 M $[Bu_4N]PF_6/CH_3CN$; CV sweep rate 0.1 V s^{-1}, except as noted. [b] Sweep rate 0.5 V s^{-1}.

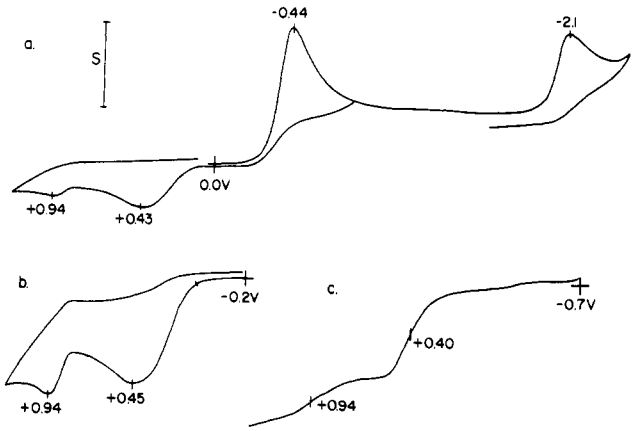

Figure 1. (a) Cyclic voltammetry of 1.17 mM $MoOCl_2(S_2CNEt_2)_2$ in 0.1 M $[Et_4N]BF_4/CH_3CN$ (ν = 0.2 V s^{-1}). (b) Cyclic voltammetry of (a) after coulometric reduction at −0.7 V (ν = 0.2 V s^{-1}). (c) Reverse pulse voltammogram of 0.69 mM $MoOCl_2(S_2CNEt_2)_2$ in 0.1 M $[Et_4N]BF_4/CH_3CN$, recorded with scan in positive direction from −0.7 V. Current sensitivity, S (at 0.02-cm^2 electrode): (a) 10 μA; (b) 10 μA; (c) 25 μA.

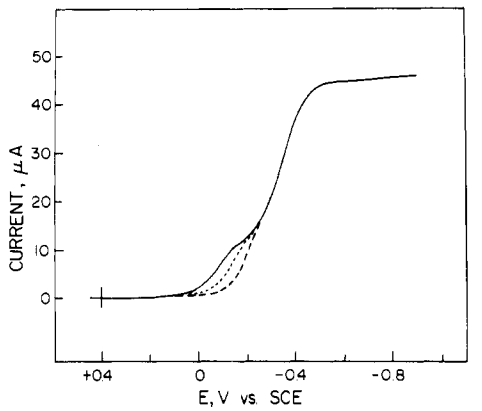

Figure 2. Normal pulse voltammetry of 1.11 mM $MoOBr_2(S_2CNEt_2)_2$: (—) in 0.1 M $[Bu_4N]PF_6/CH_3CN$; (···) in the preceding solvent mixture plus 5.6 mM $[Bu_4N]Br$; (- - -) in the preceding solvent mixture plus 18 mM $[Bu_4N]Br$.

$(S_2CNEt_2)_4^{2+}$ (+1.15 V)[17h,i] and the six-coordinate dioxo complex $MoO_2(S_2CNEt_2)_2$ (−0.93 V).[12b,i] The trend in redox potentials (Mo^{6+} > MoO^{4+} > MoO_2^{2+}) primarily reflects the number of strongly donating oxo groups coordinated to the metal; other ligands in the coordination shell exert a secondary influence on the observed value. The difference in potentials is greater between Mo^{6+} and MoO^{4+} centers than between MoO^{4+} and MoO_2^{2+} centers. This observation is explicable in terms of recent bonding descriptions of these molecules.[3,26] In MoO^{4+} two Mo dπ orbitals and one Mo dσ orbital are available to accept charge from the single oxo group, but in *cis*-MoO_2^{2+} charge from two oxo groups must be shared among three Mo dπ and two Mo dσ orbitals. Thus, a smaller increment in charge donation and a smaller change in reduction potential would be expected to result from bonding of the second oxo group.

We also observe that the seven-coordinate W(VI) complex $WOCl_2(S_2CNEt_2)_2$[7] is reduced at −1.0 V in CH_3CN. This potential is ca. 600 mV more negative than the value for $MoOCl_2(S_2CNEt_2)_2$ reduction, in line with the greater difficulty usually encountered in reducing W-containing species compared to the situation for their Mo analogues.[12d,f,27,28]

$MoOCl_2(S_2CNEt_2)_2$ and $MoOBr_2(S_2CNEt_2)_2$. Electrochemical behavior of $MoOCl_2(S_2CNEt_2)_2$ is illustrated in Figure 1. An irreversible reduction is observed for this compound at −0.4 V by both CV (Figure 1a) and NPV. The total NPV current parameter for this wave, i_d/AC = 1870 $\mu A\ cm^{-2}\ mM^{-1}$ (Table II), is consistent with a two-electron transfer (cf. Table I). This result is confirmed by controlled-potential coulometry, which yields n = 2.06 for electrolysis of **1a** at −0.7 V. The CV current parameter $i_p/\nu^{1/2}AC$ = 1550 $\mu A\ s^{1/2}\ V^{-1/2}\ cm^{-2}\ mM^{-1}$ is greater than the value for a one-electron transfer but does not accurately reflect the two-electron character of the electrode reaction for reasons that may include incomplete overlap of the individual charge-transfer steps, slow electron-transfer kinetics, and an additional small wave produced by solvolysis of the complex (vide infra). Similar behavior is observed for compound **1b** and is summarized in Table II.

The electrode reaction products of $MoOCl_2(S_2CNEt_2)_2$ and $MoOBr_2(S_2CNEt_2)_2$ are detected by extending or reversing the voltammetric sweep following the initial reduction step of these compounds. Figure 1a shows that continuation of a CV sweep to more negative values after reduction of **1a** produces a peak at −2.1 V, which we assign to reduction of $MoO(S_2CNEt_2)_2$ (Table III). Reversal of the sweep to positive values immediately after the −0.4-V reduction wave produces anodic peaks at +0.4 and +0.9 V, which coincide with the oxidations of $MoO(S_2CNEt_2)_2$ and Cl^-, respectively. A cyclic voltammogram recorded after two-electron CPC reduction of $MoOCl_2(S_2CNEt_2)_2$ also exhibits these oxidation waves (Figure 1b), as does a reverse pulse voltammogram[29] of **1a** (Figure 1c). Absence of an anodic peak near 0 V on all positive-going scans indicates that $Et_2NCS_2^-$ is not a product of $MoOCl_2(S_2CNEt_2)_2$ reduction. From these results, we conclude that the reductions of **1a** and **1b** at −0.4 V proceed by overall two-electron transfer to $MoO(S_2CNEt_2)_2$ and halide ion as described by eq 1.

$$MoOX_2(S_2CNEt_2)_2 + 2e^- \rightarrow MoO(S_2CNEt_2)_2 + 2X^- \quad (1)$$
$$X = Cl, Br$$

(26) Cotton, F. A. *Chem. Uses Molybdenum, Proc. Int. Conf., 1st* **1973**, *1*, 6–10.
(27) Callis, G. E.; Wentworth, R. A. D. *Bioinorg. Chem.* **1977**, *7*, 57.
(28) Rice, C. A.; Kroneck, P. M. H.; Spence, J. T. *Inorg. Chem.* **1981**, *20*, 1996.
(29) Osteryoung, J.; Kirowa-Eisner, E. *Anal. Chem.* **1980**, *52*, 62.

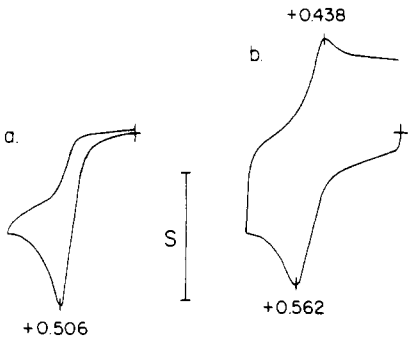

Figure 3. Cyclic voltammetry of 0.81 mM $MoO(S_2CNEt_2)_2$ in 0.1 M $[Et_4N]BF_4/CH_3CN$ (0.02-cm^2 electrode): (a) $v = 0.2$ V s^{-1}, $S = 5$ μA; (b) $v = 27$ V s^{-1}, $S = 100$ μA.

In CH_3CN solution compounds **1a** and **1b** each exhibit an additional wave at a potential 0.2–0.3 V more positive than the main reduction wave. As shown in Figure 2, this wave accounts for 25–35% of the total **1b** reduction current within 20 min of solution preparation; it increases to 80–90% of the total within 1 h. (After similar times the extra wave of **1a** is 4–5 times smaller.) Voltammetric waves corresponding to oxidation of free Br^- also are observed in solutions of **1b** and increase with time in a similar manner. The extra reduction waves vanish if excess halide ion is added to the solution. Figure 2 shows the result of addition of Br^- to a solution of $MoOBr_2(S_2CNEt_2)_2$. We attribute the observed behavior to reversible dissociation of halide ion from the Mo(VI) center and formation of either a six-coordinate monohalo or seven-coordinate solvento complex that is easier to reduce than the parent compound.[30] The solvolyzed complexes formed in eq 2 appear to undergo reduction to Mo(IV) analogously to

$$MoOX_2(S_2CNEt_2)_2 \overset{CH_3CN}{\rightleftharpoons} [MoOX(S_2CNEt_2)_2]^+ + X^- \text{ or } [MoOX(CH_3CN)(S_2CNEt_2)_2]^+ + X^- \quad (2)$$

eq 1, because we observe that the total current parameter measured by NPV for the new wave plus the main wave (see Figure 2 and Table II) remains constant and equal to the value for a two-electron transfer.

$MoO(S_2CNEt_2)_2$, the molybdenum-containing reduction product of **1a** and **1b**, is not reoxidized on reverse sweep until the potential reaches +0.4–0.5 V. At normal CV sweep rates in the absence of Cl^- this oxidation is irreversible (Figure 3a). However, at sweep rates above 5 V s^{-1} in 0.1 M $[Et_4N]BF_4/CH_3CN$ we observe a cathodic counterpart to the $MoO(S_2CNEt_2)_2$ oxidation wave (Figure 3b), which we interpret as evidence for the quasi-reversible one-electron oxidation of this compound.

$$MoO(S_2CNEt_2)_2 \rightleftharpoons [MoO(S_2CNEt_2)_2]^+ + e^- \quad (3)$$

At $v = 27$ V s^{-1} the CV parameters for eq 3 are $E^{\circ\prime} = +0.50$ V, $\Delta E_p = 125$ mV, and $i_p/v^{1/2}AC = 900$ μA $s^{1/2}$ $V^{-1/2}$ cm^{-2} mM^{-1}. The NPV current parameter for oxidation of $MoO(S_2CNEt_2)_2$ in CH_3CN is 1130 μA cm^{-2} mM^{-1} (Table III).

The current parameter measured for reaction 3 increases when chloride ion is present. For example, NPV oxidation of **4** in the presence of 10 mM Cl^- yields a total i_d/AC of 2100 μA cm^{-2} mM^{-1}. In the reverse pulse voltammogram in Figure 1c, the wave at +0.4 V (representing reoxidation of **4** in the presence of the Cl^- generated by reduction of **1a**) has a current parameter of 1700 μA cm^{-2} mM^{-1}. This is nearly equal to the value expected for a two-electron transfer in CH_3CN, indicating that the same number of electrons are transferred in the reduction and reoxidation steps.[29] Controlled-potential coulometric oxidation of **4** at +0.6 V in the presence of 10 mM Cl^- requires 1.8 faraday/mol of Mo and produces a solution with voltammetric characteristics idential with those of **1a**. Also, it is evident from Figure 1 that free Cl^- is consumed during oxidation of Mo(IV). There, the current at +0.9 V is smaller than expected if all chloride released by reduction of **1a** were to be oxidized at this potential. Thus, we conclude that free chloride ions are bound to the molybdenum center as Mo(IV) is oxidized to Mo(VI) and that electrooxidation of $MoO(S_2CNEt_2)_2$ in the presence of Cl^- is represented by eq 4.[33]

$$MoO(S_2CNEt_2)_2 + 2Cl^- \rightarrow MoOCl_2(S_2CNEt_2)_2 + 2e^- \quad (4)$$

Equations 1 and 4 are net two-electron transfers that are the chemical reverse of one another. A change of 2 in molybdenum coordination number accompanies each electrode reaction. We suggest that these changes provide the driving force that enables transfer of two electrons to occur at the same potential. In each case, loss or gain of chloride ligands compensates for the electrostatic charge transferred in the electrode reaction and facilitates transfer of the second electron. A system of coupled electron-transfer and coordination reactions that is consistent with the observed behavior is presented as Scheme I.[34]

We have attempted to verify the details of Scheme I by examining the voltammetric behavior of its individual compounds. For example, observation of quasi-reversible one-electron transfer for oxidation of **4** by fast-sweep-rate CV (eq 3) suggests that the initial step in the two-electron oxidation of $MoO(S_2CNEt_2)_2$ in

Scheme I[a]

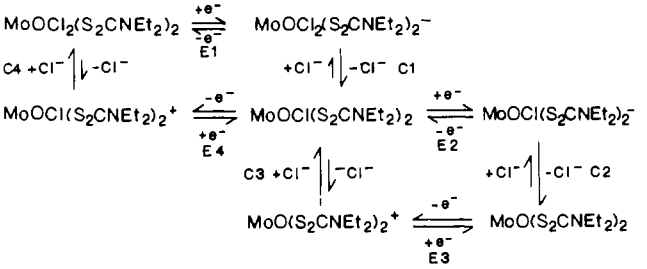

[a] Capital letters E and C refer to electrochemical and chemical reactions, respectively. The numbers following them do not necessarily refer to specific equations in the text.

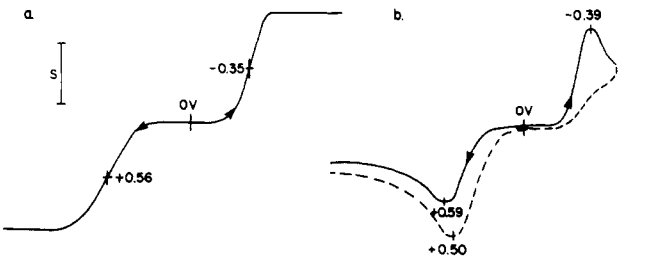

Figure 4. (a) Oxidative and reductive NPV of 3.4 mM $MoOCl(S_2CNEt_2)_2$ in 0.1 M $[Bu_4N]PF_6/CH_3CN$ ($S = 400$ μA, 0.2-cm^2 electrode). (b) Oxidative and reductive CV of 1.25 mM $MoOCl(S_2CNEt_2)_2$ in 0.1 M $[Bu_4N]PF_6/CH_3CN$ ($v = 0.5$ V s^{-1}, $S = 80$ μA, 0.2 cm^2 electrode; broken line illustrates the additional anodic current at 0.5 V that results from scan reversal after cathodic sweep).

(30) Other examples of solvolytic replacement of halide ion by CH_3CN result in similar changes in metal-centered reduction potentials. For example, $WCl_2H_2(PMe_3)_4$ and $WCl(CH_3CN)H_2(PMe_3)_4^+$ exhibit a difference of 0.5 V in reduction potential[31] and $[Ru(NH_3)_5Cl]^{2+}$ and $[Ru(NH_3)_5(CH_3CN)]^{3+}$ a difference of 0.4 V.[32]

(31) Sharp, P. R.; Frank, K. G. *Inorg. Chem.* **1985**, *24*, 1808.

(32) Matsubara, T.; Ford, P. C. *Inorg. Chem.* **1976**, *15*, 1107.

(33) We have not attempted to verify the analogous process for bromide ion because of the proximity of the Br^- and $MoO(S_2CNEt_2)_2$ oxidation waves.

(34) Scheme I is an example of a "scheme of squares",[35] which is widely used to interpret multielectron electrode reactions consisting of coupled proton and electron transfers. Such a scheme is readily adapted to multielectron transfer based on coordination reactions or other processes involving a change in molecular structure.

(35) (a) Jacq, J. *Electrochim. Acta* **1967**, *12*, 1345. (b) Albery, W. J.; Hitchman, M. L. *Ring-Disc Electrodes*; Oxford University Press: Oxford, England, 1971; Chapter 5. (c) Laviron, E. *J. Electroanal. Chem. Interfacial Electrochem.* **1983**, *146*, 15. (d) Bond, A. M.; Oldham, K. B. *J. Phys. Chem.* **1983**, *87*, 2492.

the presence of Cl^- is likely to be reaction E3 in Scheme I. However, we have been unable to detect the initial step in the two-electron reduction of **1a** or an anodic counterpart to the −0.4 V reduction wave, which could be assigned to Mo(V) → Mo(VI) reoxidation. Cyclic voltammetry of **1a** at low temperature (0 °C), at fast sweep rates (ν = 1–270 V s^{-1}), and in the presence of 0.1 M Cl^- reveals only a 15–40% decrease in $i_p/\nu^{1/2}AC$ at sweep rates above 1 V s^{-1} in the presence of 0.1 M Cl^-. In view of the small extent and slow rate of Cl solvolysis exhibited by $MoOCl_2(S_2CNEt_2)_2$ in eq 2, it is likely that the first step in the reduction of **1a** is electrochemical (reaction E1) rather than chemical (reaction C4). However, the remaining steps in the reaction sequence apparently occur with such speed that only an overall two-electron transfer is observed.

To further verify Scheme I, we examined the electrochemistry of **5**,[7] the six-coordinate Mo(V) complex that occupies a central position in the redox chemistry of these compounds. As illustrated by Figure 4 and the data in Table III, compound **5** undergoes an irreversible one-electron reduction at −0.35 V. $MoO(S_2CNEt_2)_2$ is detected as a product of this reduction by its voltammetric wave at −2.1 V (not shown). Therefore, we conclude that that electrochemical reduction of **5** proceeds by the reaction

$$MoOCl(S_2CNEt_2)_2 + e^- \rightarrow MoO(S_2CNEt_2)_2 + Cl^- \quad (5)$$

Since the potential of eq 5 is slightly more positive than that of eq 1, compound **5**, if formed as an intermediate in the reduction of **1a**, would be immediately reduced to $MoO(S_2CNEt_2)_2$ plus Cl^-, resulting in the two-electron transfer described by eq 1.

Figure 4 and Table III show that **5** also undergoes a one-electron oxidation at +0.56 V, which we assign to the electrode reaction

$$MoOCl(S_2CNEt_2)_2 \rightarrow MoOCl(S_2CNEt_2)_2^+ + e^- \quad (6)$$

Thus, if $MoOCl(S_2CNEt_2)_2$ were formed by oxidation of **4** plus addition of Cl^-, it could be oxidized at a slightly more positive potential and add a second Cl^- to give $MoOCl_2(S_2CNEt_2)_2$, resulting in an overall two-electron transfer at +0.4–0.6 V.[36]

Scheme I illustrates how multielectron transfer can occur at mononuclear MoO^{4+}, MoO^{3+}, and MoO^{2+} centers by coupling of coordination and electron-transfer reactions. The coordination steps are formulated as metal–ligand bond-forming or bond-breaking reactions that are displaced in the direction of the large arrows. We expect that $MoOCl_2(S_2CNEt_2)_2$ reduction follows the pathway E1–C1–E2–C2 and $MoO(S_2CNEt_2)_2$ oxidation the pathway E3–C3–E4–C4. Because of the irreversible nature of the chemical reactions, electrochemical interconversion of $MoOCl_2(S_2CNEt_2)_2$ and $MoO(S_2CNEt_2)_2$ is highly irreversible. A separation of 0.8–1.0 V exists between the potentials of Mo(VI) reduction and Mo(IV) oxidation for these species. An issue yet to be resolved is whether the electron-transfer and coordination reactions occur as discrete events in all cases. In the case of $MoO(S_2CNEt_2)_2$ oxidation, it appears that Cl^- coordination occurs as a discrete step after charge transfer. However, in the reductions of **1a**, **1b**, and **5**, metal–ligand bond breaking may occur so rapidly as to be indistinguishable from an event simultaneous with charge transfer. Further mechanistic studies are needed to answer this question.

The probable pathways of reduction and reoxidation in Scheme I lead to the conclusion that the following changes in Mo oxidation state and coordination number (CN) occur during electron transfer: Mo(VI) (CN = 7) → Mo(V) (CN = 6) → Mo(IV) (CN = 5). This sequence of changes is consistent with coordination numbers typically exhibited by MoO^{4+}, MoO^{3+}, and MoO^{2+} species.[3] We explain its existence on the following basis. Reduction of Mo(VI) to Mo(V) results in half-filling of the Mo $4d_{xy}$ orbital, which, because of the strong electronic influence of the apical oxo group, is constrained to lie in the equatorial plane. In pentagonal-bipyramidal geometry the four lobes of this orbital cannot all be directed away from five coplanar bonding electron pairs. Consequently, electrochemical reduction results in half-filling of what is effectively an antibonding orbital and cleavage of one of the equatorial bonds ensues. For **1a** and **1b** reduction, this is a bond to a halide ligand. Subsequent reduction of $MoOCl(S_2CNEt_2)_2$ requires that a second electron be added to the same d_{xy} orbital. $MoOCl(S_2CNEt_2)_2$ and the square-pyramidal $MoO(S_2CNEt_2)_2$ product have the same number of ligands in the *xy* plane. Thus, electrostatic rather than orbital interactions would appear to be responsible for cleavage of the metal–ligand bond in conjunction with the second electron transfer.

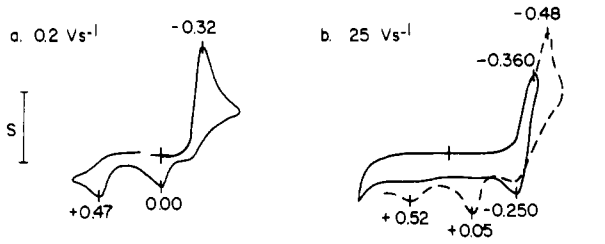

Figure 5. Cyclic voltammetry of 0.68 mM $[MoO(S_2CNEt_2)_3]BPh_4$ in 0.1 M $[Et_4N]BF_4/CH_3CN$ (0.02-cm^2 electrode): (a) ν = 0.2 V s^{-1}, S = 5 μA; (b) ν = 25 V s^{-1}, S = 50 μA.

Table IV. Cyclic Voltammetric Data for $[MoO(S_2CNEt_2)_3]^+$ Reduction[a]

ν, V s^{-1}	$E_{pc}(1)$, V	$E_{pc}(2)$, V	$i_{pc}/\nu^{1/2}AC$, μA $s^{1/2}$ $V^{-1/2}$ cm^{-2} mM^{-1}	$E^{\circ\prime}$, V (ΔE_p, mV)[d]
0.02	−0.286		1419[b]	
0.05	−0.300		1416[b]	
0.1	−0.308		1396[b]	
0.2	−0.325		1342[b]	
0.4	−0.338		1280[b]	
5	−0.347	−0.428	976[c]	−0.304 (96)
25	−0.360	−0.476	791[c]	−0.305 (110)
75	−0.380	−0.501	767[c]	−0.318 (124)
110	−0.389	−0.521	750[c]	−0.312 (170)

[a] 0.68 mM $[MoO(S_2CNEt_2)_3]BPh_4$ in 0.1 M $[Et_4N]BF_4/CH_3CN$. [b] Merged wave, total current function reported. [c] Split wave, current function for first wave reported. [d] $E^{\circ\prime} = {}^1/_2(E_{pc} + E_{pa})$, and $\Delta E_p = E_{pa} - E_{pc}$ for first wave.

$[MoO(S_2CNEt_2)_3]^+$. To demonstrate the possible existence of reversible Mo(VI)/Mo(V) electrochemistry at MoO^{4+} centers, we extended our investigation to the tris(bidentate) complex **2**. This compound undergoes an irreversible reduction at −0.32 V, which is determined to be a two-electron transfer on the basis of its NPV current parameter (i_d/AC = 1760 μA cm^{-2} mM^{-1}, Table II). Figure 5a shows a cyclic voltammogram of **2** recorded at 0.2 V s^{-1}. When the sweep is reversed after the −0.32 V reduction wave, anodic peaks are observed at 0.00 and +0.47 V, which correspond to the oxidation of free $Et_2NCS_2^-$ and $MoO(S_2CNEt_2)_2$, respectively. Therefore, reduction of **2** at slow sweep rates proceeds by the reaction

$$[MoO(S_2CNEt_2)_3]^+ + 2e^- \rightarrow MoO(S_2CNEt_2)_2 + Et_2NCS_2^- \quad (7)$$

At fast sweep rates, this two-electron transfer is resolved into sequential one-electron steps, as shown by the CV recorded at 25 V s^{-1} in Figure 5b. If the sweep is reversed after the first of these waves (solid line, Figure 5b), a single anodic peak corresponding to Mo(V) to Mo(VI) oxidation is observed at −0.25 V. Peaks for $Et_2NCS_2^-$ and $MoO(S_2CNEt_2)_2$ oxidation are *not* observed on this trace, but they are if the negative sweep is extended beyond the second reduction wave before reversal (broken line, Figure 5b). Therefore, at fast sweep rates, **2** undergoes reversible Mo-

(36) Inasmuch as eq 6 occurs at a slightly more positive potential than eq 3 (cf. Table III), oxidation of $MoO(S_2CNEt_2)_2$ via eq 4 may occur by two overlapping 1e steps rather than a single 2e transfer. This possibility is supported by the breadth of the Mo(IV) → Mo(VI) oxidation waves in parts a and b of Figure 1, which at 0.2 V s^{-1} have shape parameters of $E_p - E_{p/2}$ = 180 and 200 mV, respectively, compared to $E_p - E_{p/2}$ = 90 mV for oxidation of $MoO(S_2CNEt_2)_2$ in the absence of Cl^- at the same sweep rate. Noncoincidence of the Mo(IV) → Mo(V) and Mo(V) → Mo(VI) oxidation steps also is indicated by noncoincidence of the anodic peak potentials for the two traces shown in Figure 4b.

Scheme II

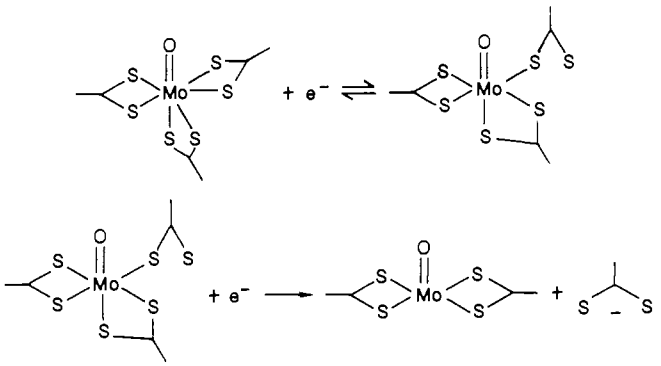

(VI)/Mo(V) reduction followed by irreversible Mo(V)/Mo(IV) reduction:

$$[MoO(S_2CNEt_2)_3]^+ + e^- \rightleftharpoons MoO(S_2CNEt_2)_3 \quad (8)$$

$$MoO(S_2CNEt_2)_3 + e^- \rightarrow MoO(S_2CNEt_2)_2 + Et_2NCS_2^- \quad (9)$$

Since reaction 9 is irreversible, it shifts to positive potentials with decreasing sweep rate and ultimately overlaps eq 8 to give the irreversible two-electron behavior of eq 7. Cyclic voltammetric data illustrating this behavior are presented in Table IV. A formal potential of $E^{\circ\prime} = -0.31$ V is calculated for eq 8 from the fast-sweep-rate data.

We believe that electrochemical reduction of **2** follows the same changes in Mo oxidation state and coordination number described previously for compounds **1a** and **1b**. However, when three bidentate ligands are coordinated to the MoO^{4+} center, cleavage of a single metal–ligand bond does not lead to chemically irreversible behavior because the ligand is not displaced from the molecule, and the bond readily re-forms upon reoxidation to Mo(VI). Consequently, a chemically reversible Mo(VI)/Mo(V) redox couple is observed for complex **2** (Figure 5b). Reduction of Mo(IV) is irreversible because cleavage of a second metal–ligand bond displaces a bidentate ligand from the molecule. The full electrochemical behavior of $[MoO(S_2CNEt_2)_3]^+$ is depicted in Scheme II. As described above, we presume that a bond in the equatorial plane is broken by partial occupancy of the Mo $4d_{xy}$ orbital in conjunction with Mo(VI) to Mo(V) reduction. This results in a six-coordinate complex with a monodentate dithiocarbamate ligand. There is precedence for structures of this type in the compounds $Ru(NO)(S_2CNEt_2)_3$[37] and $Re(NR)(S_2CNEt_2)_3$.[38] In these cases, existence of six-coordinate geometry with one monodentate $Et_2NCS_2^-$ group apparently is enforced by the d-orbital occupancy of the metal.

In contrast to the case for all other MoO^{4+} complexes examined in this paper, controlled-potential coulometric reduction of **2** on the plateau of its two-electron reduction wave results in an apparent n value of 0.89 (Table II). Since two-electron behavior is observed by CV and NPV, one or more slow chemical reactions must occur during the lengthier coulometry experiment to give $n = 1$. NPV analysis of the rose-colored solution produced by coulometric reduction of **2** reveals anodic waves at $E_{1/2} = +0.44$ and +0.88 V with $i_d/AC = 1070$ and 2080 $\mu A\ cm^{-2}\ mM^{-1}$, respectively, and overlapping cathodic waves between −0.85 and −1.1 V with a total i_d/AC value of 480 $\mu A\ cm^{-2}\ mM^{-1}$. No wave is observed for $Et_2NCS_2^-$ oxidation. The current parameter of the anodic wave at +0.44 V is consistent with quantitative generation of $MoO(S_2CNEt_2)_2$ by two-electron reduction of **2**. We have not attempted to characterize the other species produced by electrochemical reduction of **2** nor the chemical reactions responsible for the coulometric result of $n = 1$.

MoO(cat)$(S_2CNEt_2)_2$. The $MoO(cat)(S_2CNEt_2)_2$ complexes (**3**) also have tris(bidentate) coordination about an MoO^{4+} center.

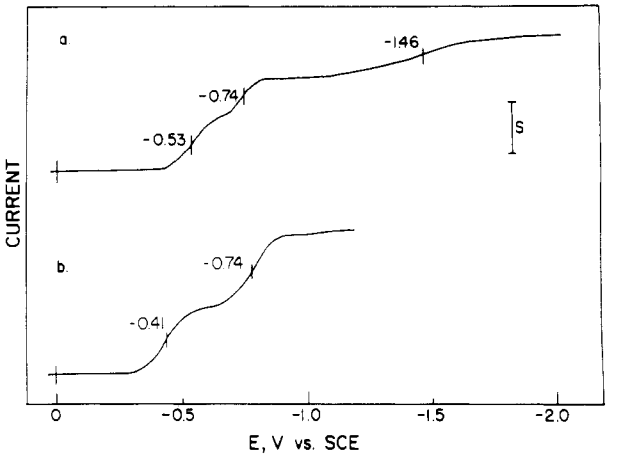

Figure 6. Normal pulse voltammetry (0.2-cm^2 electrode): (a) 0.29 mM $MoO(Cl_4cat)(S_2CNEt_2)_2$ in 0.1 M $[Bu_4N]PF_6/CH_3CN$ ($S = 50\ \mu A$); (b) 1.15 mM $MoO(Cl_4cat)(S_2CNEt_2)_2$ in 0.1 M $[Bu_4N]PF_6$/DMF ($S = 100\ \mu A$).

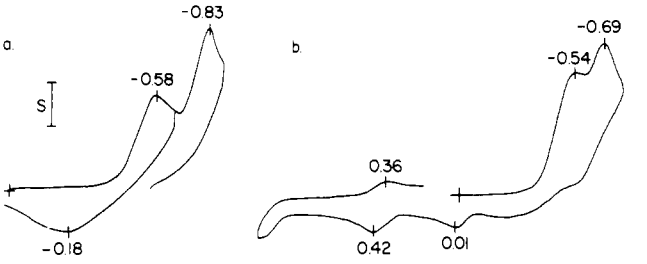

Figure 7. Cyclic voltammetric reduction (0.02-cm^2 electrode): (a) 0.75 mM $MoO(Cl_4cat)(S_2CNEt_2)_2$ in 0.1 M $[Bu_4N]PF_6$/DMF ($\nu = 2.3\ V\ s^{-1}$, $S = 4\ \mu A$); (b) 0.89 mM $MoO(Cl_4cat)(S_2CNEt_2)_2$ in 0.1 M $[Et_4N]BF_4/CH_3CN$ ($\nu = 0.2\ V\ s^{-1}$, $S = 2\ \mu A$).

We investigated these compounds to determine if further examples of reversible Mo(VI)/Mo(V) electrochemistry could be found and to examine the effect of the electronically different catechol ligand on the two-electron reduction of MoO^{4+} species. Among the nine $MoO(cat)(S_2CNEt_2)_2$ complexes that have been prepared,[18] we report here results for those with $cat^{2-} = Cl_4cat^{2-}$ (**3a**), NO_2cat^{2-} (**3b**), Cat^{2-} (**3c**), and $DTBcat^{2-}$ (**3d**). These complexes display one of two patterns of behavior depending on whether the catechol ligands contain relatively electron withdrawing (**3a,b**) or electron donating (**3c,d**) substituents. Results for **3a–d** are representative of the full range of behavior exhibited by $MoO(cat)(S_2CNEt_2)_2$ complexes. Findings for the entire series of compounds are reported in a subsequent paper.[18]

Figure 6a illustrates the NPV reduction of $MoO(Cl_4cat)(S_2CNEt_2)_2$ in CH_3CN. Cathodic waves with $i_d/AC = 940$ and 550 $\mu A\ cm^{-2}\ mM^{-1}$ are observed at −0.53 and −0.74 V, respectively. The current parameter measured on the plateau of the second wave is smaller than expected for a two-electron transfer, and CPC reduction of **3a** at this potential yields $n = 1.75$ (Table II). Continuation of the NP voltammogram to more negative potentials reveals a third wave at ca. −1.5 V and a total parameter of 1840 $\mu A\ cm^{-2}\ mM^{-1}$, which is consistent with two-electron transfer. **3b** exhibits similar behavior (Table II), but its most negative reduction wave is obscured by NO_2 group reduction.

Simpler electrochemical behavior is observed for these two compounds in other solvents. Figure 6b shows the NPV reduction of **3a** in DMF. Two cathodic waves of equal height are observed, each having a current parameter consistent with one-electron transfer in this solvent, $i_d/AC = 560$ and 550 $\mu A\ cm^{-2}\ mM^{-1}$. A similar result is obtained in CH_2Cl_2 (Table II). Figure 7a shows that reduction of **3a** in DMF by CV at 2.3 $V\ s^{-1}$ also results in two one-electron reduction waves ($i_p/\nu^{1/2}AC = 410$ and 440 $\mu A\ s^{1/2}\ V^{-1/2}\ cm^{-2}\ mM^{-1}$, respectively). If the sweep is reversed after the first wave, an anodic peak corresponding to Mo(V) → Mo(VI) reoxidation is observed at −0.18 V; no other waves are observed

(37) Domenicano, A.; Vaciago, A.; Zambonelli, L.; Loader, P. L.; Venanzi, L. M. *J. Chem. Soc., Chem. Commun.* **1966**, 476.
(38) Goeden, G. V.; Haymore, B. L. *Inorg. Chem.* **1983**, *22*, 157.

Scheme III

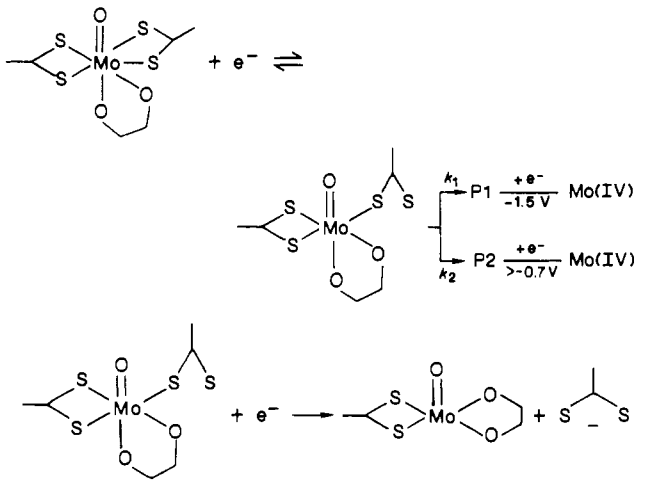

if the reverse sweep is continued to more positive potentials. However, if the negative scan is extended through the second reduction wave before reversal, diminished current is observed for Mo(V) → Mo(VI) oxidation at −0.18 V, and additional waves corresponding to irreversible oxidation of $Et_2NCS_2^-$ at 0.0 V and reversible oxidation of Mo(IV) at +0.4 V appear on the reverse sweep (Figure 7b). There is no evidence for release of the catechol ligand, which would be detectable from waves for the $cat^{2-}/SQ^{\bullet-}$ and $SQ^{\bullet-}/Q$ redox couples of these species.[39]

We conclude from these results that reduction of **3a** and **3b** in DMF and CH_2Cl_2 occurs by the following one-electron steps. These reactions are represented in Scheme III.

$$MoO(cat)(S_2CNEt_2)_2 + e^- \rightleftharpoons [MoO(cat)(S_2CNEt_2)_2]^- \quad (10)$$

$$[MoO(cat)(S_2CNEt_2)_2]^- + e^- \rightarrow [MoO(cat)(S_2CNEt_2)]^- + Et_2NCS_2^- \quad (11)$$

Equations 10 and 11 are analogous to eq 8 and 9 for $MoO(S_2CNEt_2)_3^+$ reduction and likely involve a similar sequence of changes in Mo oxidation state and coordination number; i.e., Mo(VI) (CN = 7) → Mo(V) (CN = 6) → Mo(IV) (CN = 5). One feature arising from the presence of cat^{2-} in the MoO^{4+} coordination shell is a difference of 0.2–0.3 V between the potentials of Mo(VI)/Mo(V) and Mo(V)/Mo(IV) reduction. Consequently, better resolution of these one-electron transfers is obtained for the $MoO(cat)(S_2CNEt_2)_2$ complexes than for $MoO(S_2CNEt_2)_3^+$. Since $Et_2NCS_2^-$ is the ligand ultimately displaced from $MoO(cat)(S_2CNEt_2)_2$, we believe that a Mo–S bond is broken during the first electron transfer and that the product of eq 10 is a six-coordinate Mo(V) intermediate with a monodentate dithiocarbamate as shown in Scheme III.

The Mo(IV) complex produced in eq 11 is characterized by an oxidation wave at ca. +0.4 V, which is detected on the anodic sweep of CV experiments (Figure 7b). Its oxidation occurs at a potential less positive than that of $MoO(S_2CNEt_2)_2$ (eq 3) and is reversible at slow CV sweep rates. We assign this oxidation to the electrode reaction

$$[MoO(cat)(S_2CNEt_2)]^- \rightleftharpoons MoO(cat)(S_2CNEt_2) + e^- \quad (12)$$

Formal potentials of +0.39, 0.35, and 0.41 V (determined by CV) are measured for eq 12 for the Cl_4cat^{2-}, NO_2cat^{2-}, and Cat^{2-} species, respectively. An irreversible oxidation at +0.30 V is observed for the $DTBcat^{2-}$ complex.

Although **3a** and **3b** undergo sequential one-electron reductions as illustrated by their NPV and fast-sweep-rate CV behavior in DMF and CH_2Cl_2, there is an additional feature in the electrochemistry of these compounds. Figure 6a shows that the height of the second NPV reduction wave of **3a** in CH_3CN is smaller

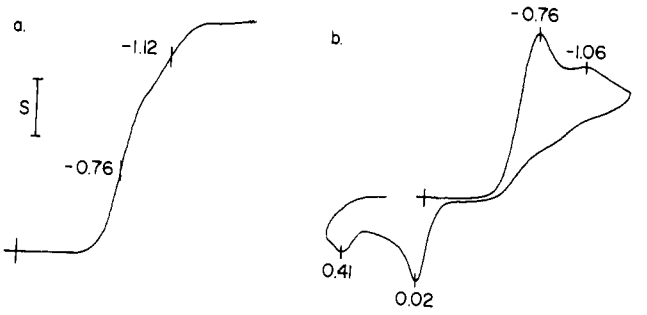

Figure 8. (a) NPV and (b) CV at 0.05 V s^{-1} of 1.02 mM $MoO(Cat)(S_2CNEt_2)_2$ in 0.1 M $[Bu_4N]PF_6/CH_3CN$ (S = (a) 100 and (b) 14.2 μA; 0.2 cm^2 electrode).

than expected for a one-electron transfer and that a third reduction wave is located at ca. −1.5 V. This behavior also is observed by slow-sweep-rate CV in CH_3CN, DMF, and CH_2Cl_2 as indicated by the data in Table II. CPC reduction of **3a** and **3b** on the plateau on the second reduction wave results in $n < 2$. We conclude for complexes **3a** and **3b** that the product of eq 10 undergoes a chemical reaction which simultaneously consumes material that is electroactive at −0.7 V and produces material that is reducible at −1.5 V.[40] The nature of the reaction is unknown, but bimolecular character is indicated by the fact that the apparent reaction rate (observed by slow-sweep-rate CV) increases with increasing complex concentration. However, we have insufficient data to characterize the reaction further. In Scheme III we identify this behavior as pathway 1, which leads to product P1 with rate constant k_1. Pathway 1 is followed by all $MoO(cat)(S_2CNEt_2)_2$ complexes with electron-withdrawing catechol substituents (**3a**, **3b**, and $MoO(Br_4cat)(S_2CNEt_2)_2$[18]). The rate of the reaction leading to P1 is solvent-dependent; k_1 is appreciably larger in CH_3CN than in DMF or CH_2Cl_2. In the last two solvents the effect of the reaction is observed only by slow-sweep-rate CV, but in CH_3CN k_1 is large enough to influence behavior on the NPV time scale.

Compounds **3c** and **3d** typify the behavior of complexes bearing catechol ligands with electron-donating or nonwithdrawing substituents. As illustrated by NPV of **3c** in Figure 8a, these compounds exhibit reduction waves at −0.7 and −1.1 V in CH_3CN. The current parameter on the plateau of the first wave lies between the values for one- and two-electron transfer in this solvent but increases to a value consistent with two-electron stoichiometry on the plateau of the second wave (i_d/AC = 1850–1900 μA cm^{-2} mM^{-1}, Table II). CPC reduction at this more negative potential yields n = 2.16 and 2.09 for **3c** and **3d**, respectively. Slow-sweep-rate CV (Figure 8b) shows a large reduction at −0.7 V and a smaller peak at −1.1 V. Anodic peaks at 0.0 V ($Et_2NCS_2^-$ oxidation) and +0.4 V (Mo(IV) oxidation) are observed on scan reversal.

We have not isolated the primary electron-transfer event associated with **3c** and **3d** reduction. We assume that eq 10 and 11 represent the principal reduction steps of these compounds. In contrast to the behavior of **3a** and **3b**, the relative magnitudes of the −0.7 and −1.1 V reduction waves suggest that the initial reduction products of **3c** and **3d** undergo chemical reactions which produce species that are reducible at the potential of the first wave. This behavior, which is designated as pathway 2 in Scheme III, is characterized by rate constant k_2 and product P2. Our failure to observe the primary electron-transfer event indicates that $k_2 > k_1$. Comparison of relative magnitudes of the first NPV reduction wave reveals also that k_2 exhibits a solvent dependence (CH_2Cl_2 > CH_3CN > DMF) and increases with increasing electron donor strength of the catechol substituents. These effects combine to cause $MoO(DTBcat)(S_2CNEt_2)_2$ reduction in CH_2Cl_2 to appear as single two-electron transfer by both CV and NPV (Table II).

(39) Potentials of the $cat^{2-}/SQ^{\bullet-}$ and $SQ^{\bullet-}/Q$ redox couples are given in Table IV of the accompanying article.[18]

(40) Alternately, reaction between the Mo(IV) electrode product and Mo(VI) reactant could lead to the same result.

The foregoing results illustrate several effects of the catechol ligand on electrochemical behavior of MoO^{4+} complexes. First, the electron-donating character of catechol shifts the Mo(VI) reduction potential to more negative values and increases the separation between the potentials of Mo(VI)/Mo(V) and Mo(V)/Mo(IV) reduction. These effects increase with increasing donor strength of the catechol substituents. The net result is that the separation between Mo(VI)/Mo(V) and Mo(V)/Mo(IV) potentials increases from effectively 0 V in compounds **1a** and **1b** to ca. 0.4 V in compounds **3c** and **3d** while the Mo(VI) reduction potential itself shifts negatively by about 0.4 V. The electronic character of the catechol substituents also influences the mechanism of $MoO(cat)(S_2CNEt_2)_2$ reduction. When electron-withdrawing substituents are present, a concentration-dependent reaction occurs that consumes species undergoing reduction at the potential of the second wave and produces a material that is reducible at a more negative potential. When electron-donating or nonwithdrawing substituents are present, a different reaction ensues that causes more than one electron to be transferred at the potential of the first reduction wave. We do not know the mechanisms or products of these chemical reactions. Voltammetric analyses of solutions prepared by coulometric reduction of **3a-d** reveal large waves for oxidation of $Et_2NCS_2^-$, but no indication of the Mo(IV) complexes described in eq 3 and 12 nor of free catecholate ligands. Presumably, the ultimate reduction products are molybdenum catecholate species.

Acknowledgment. We are pleased to acknowledge support of this research by the National Science Foundation under Grant No. CHE-84-09594.

Registry No. **1a**, 57146-54-0; **1b**, 53548-92-8; **2**, 58760-67-1; **2**·BPh_4, 104598-32-5; **3a**, 104574-85-8; **3b**, 104574-86-9; **3c**, 104574-84-7; **3d**, 104574-87-0; **4**, 25395-92-0; **5**, 67673-25-0; $[MoO(Cl_4cat)(S_2CNEt_2)_2]^-$, 104574-88-1; $[MoO(Cl_4cat)(S_2CNEt_2)]^-$, 104574-89-2; $[MoO(NO_2cat)(S_2CNEt_2)_2]^-$, 104575-90-8; $[MoO(NO_2cat)(S_2CNEt_2)]^-$, 104574-90-5; $[MoO(cat)(S_2CNEt_2)]^-$, 104574-91-6; $MoO(Cl_4cat)(S_2NEt_2)$, 104574-92-7; $MoO(NO_2cat)(S_2CNEt_2)$, 104574-93-8; $MoO(cat)(S_2CNEt_2)$, 104574-94-9; $Na[S_2CNEt_2]$, 148-18-5; $[Et_4N]Cl$, 56-34-8; $[(heptyl)_4N]Br$, 4368-51-8; Cl^-, 16887-00-6; CH_3CN, 75-05-8.

Contribution from the Department of Chemistry, Florida Atlantic University, Boca Raton, Florida 33431

Synthesis and Properties of Seven-Coordinate (Catecholato)bis(dithiocarbamato)oxomolybdenum(VI) Complexes Exhibiting Metal- and Ligand-Centered Electrochemistry

Julie R. Bradbury[1] and Franklin A. Schultz*

Received August 23, 1985

Seven-coordinate complexes containing two diethyldithiocarbamate and one of nine different catecholate (cat) ligands bound to oxomolybdenum(VI) (MoO^{4+}) are prepared by two synthetic routes: (i) oxidative addition of *o*-quinone to oxomolybdenum(IV) ($MoO(S_2CNEt_2)_2$) and (ii) replacement of an oxo ligand by catechol on dioxomolybdenum(VI) ($MoO_2(S_2CNEt_2)_2$). These $MoO(cat)(S_2CNEt_2)_2$ complexes undergo electron-transfer reactions that encompass the Mo(VI), -(V), and -(IV) oxidation states of the metal and the catecholate, semiquinone (SQ), and quinone (Q) oxidation levels of the ligand. The electronic character of the catechol ligand influences the mechanism of metal-centered reduction. Complexes with electron-withdrawing catechol substituents undergo reduction in two one-electron steps separated by 0.2-0.3 V in CH_2Cl_2. Compounds with nonwithdrawing or electron-donating substituents also undergo separate Mo(VI)/Mo(V) and Mo(V)/Mo(IV) reductions, but a rapid chemical reaction in conjunction with charge transfer causes more than one electron to be transferred at the potential of the first wave. The ligand-centered oxidations of the $MoO(cat)(S_2CNEt_2)_2$ complexes occur at potentials ca. 1.7 V more positive than the $cat^{2-} \rightarrow SQ^{\bullet-}$ and $SQ^{\bullet-} \rightarrow Q$ oxidations of the free ligands. Such large differences reflect a strong electrostatic interaction between the oxomolybdenum(VI) center and the catechol. A strong interaction is required to compensate for unfavorable electron-transfer energetics (calculated on the basis of redox potentials to be as large as 3.6 V) between $MoO(S_2CNEt_2)_2$ and Q and to provide the necessary driving force for the two-electron oxidative-addition reaction (i) by which five of the nine complexes are formed. The solution EPR spectrum of the one-electron-oxidized product of the 3,5-di-*tert*-butylcatecholate complex exhibits coupling constants of 3.6 G to the C-4 ring proton and 2.2 G to Mo consistent with its assignment as the coordinated semiquinone, $[MoO(DTBSQ)(S_2CNEt_2)_2]^+$.

Introduction

Interest in metal-catecholate complexes[2] is stimulated by knowledge that interactions of this type occur in microbial iron transport reagents,[3] dioxygenase enzymes,[4] and electron-transfer pathways in bacterial photosynthesis.[5] Current research objectives include investigation of ligand-centered redox processes[6-14] and metal-semiquinone interactions.[15-22] Redox-active ligands on Mo are of interest with regard to the molybdenum hydroxylases,[23]

(1) Current address: Department of Chemistry, Washington University, St. Louis, MO 63130.
(2) Pierpont, C. G.; Buchanan, R. M. *Coord. Chem. Rev.* **1981**, *38*, 45.
(3) Raymond, K. N.; Carrano, C. J. *Acc. Chem. Res.* **1979**, *12*, 183.
(4) Que, L., Jr. *Struct. Bonding (Berlin)* **1980**, *40*, 39.
(5) Wraight, C. A. *Photochem. Photobiol.* **1979**, *30*, 767.
(6) Rohrscheid, F.; Balch, A. L.; Holm, R. H. *Inorg. Chem.* **1966**, *5*, 1542.
(7) (a) Sohn, Y. S.; Balch, A. L. *J. Am. Chem. Soc.* **1972**, *94*, 1144. (b) Balch, A. L. *J. Am. Chem. Soc.* **1973**, *95*, 2723. (c) Girgis, A. Y.; Sohn, Y. S.; Balch, A. L. *Inorg. Chem.* **1975**, *14*, 2327.
(8) Wicklund, P. A.; Brown, D. G. *Inorg. Chem.* **1976**, *15*, 396.
(9) Sofen, S. R.; Ware, D. C.; Cooper, S. R.; Raymond, K. N. *Inorg. Chem.* **1979**, *18*, 324.
(10) (a) Downs, H. H.; Buchanan, R. M.; Pierpont, C. G. *Inorg. Chem.* **1979**, *18*, 1734. (b) Buchanan, R. M.; Claflin, J.; Pierpont, C. G. *Inorg. Chem.* **1983**, *22*, 2552.
(11) Lauffer, R. B.; Heistand, R. H., II; Que, L., Jr. *J. Am. Chem. Soc.* **1981**, *103*, 3947.
(12) (a) Jones, S. E.; Leon, L. E.; Sawyer, D. T. *Inorg. Chem.* **1982**, *21*, 3692. (b) Chin, D. H.; Sawyer, D. T.; Schaefer, W. P.; Simmons, C. J. *Inorg. Chem.* **1983**, *22*, 752. (c) Harmalker, S.; Jones, S. E.; Sawyer, D. T. *Inorg. Chem.* **1983**, *22*, 2790.
(13) Bowmaker, G. A.; Boyd, P. D. W.; Campbell, G. K. *Inorg. Chem.* **1982**, *21*, 2403.
(14) Pell, S. D.; Salmonson, R. B.; Abelleira, A.; Clarke, M. J. *Inorg. Chem.* **1984**, *23*, 385.

0020-1669/86/1325-4416$01.50/0